Proceedings of the International Seminar on Mineral Processing Technology - 2006, Chennai, India. pp. 218 - 225.

Discrete Element Method (DEM) Analysis of Non-Cohesive Granular Material Flow in Hoppers

Amlan Datta and **B.K. Mishra**[1]

Tata Research Development and Design Centre (TRDDC), 54-B Hadapsar Industrial Estate, Pune - 411013, India
[1] Regional Research Laboratory, Bhubneshwar, Orissa
Email: amlan.datta@tcs.com

Abstract

Hoppers, silos and bins are expected to store material and provide unrestricted and uniform flow of the same in material processing plants. Traditionally, the material flow from hopper is analyzed assuming the solid mass as continuum. However, the behavior of particulate solids deviates significantly from a continuous system, due to fluctuation in its bulk material properties (e.g. bulk density) throughout the process. In the present work, a numerical technique called discrete element method (DEM) is used to analyze granular material flow from hopper. DEM tracks the trajectories of individual particles as they interact with their neighboring particles and hopper walls. These interactions ultimately translate to the overall displacement of the particles. The scheme is repeated in small time intervals covering the complete duration of the process. Here the simulations are limited to non-cohesive spherical granular material. Material flow is studied as a function of hopper geometry. This article involves visualization and flow rate analysis of coarse particles for different hopper design.

INTRODUCTION

Hoppers and bins are used in different parts of material processing plants. Besides being just storage units they are also often used to provide the surge-capacity between two unit operations. Hoppers are designed to provide unrestricted and uniform flow of material. This is, particularly, more important issue when particulate and granular materials are handled since their behavior is less predictable as compared to gases and liquid. Hence, unsteady flow is often encountered while processing granular solids.

The design of hopper is very much a function of material properties such as particle size distribution, particle density (true density and bulk density), cohesion of particles, particle shape so on and so forth. Jenike (1964) established a widely used method of designing hoppers based on the flow properties of material.

Correlating discharge flow rate with hopper design has attracted considerable attention for many years now. A very good review on this subject is written by Neddermann et al. (1982). The current research was inspired by the work of Baverloo et al. (1961) where it was shown that the mass flow rate is given by the following expression –

$$W = C_{FB}\rho_b\sqrt{g}(D-kd)^{5/2}, g/\min \quad (1)$$

Where, W is mass flow rate in g/min, D and d are the orifice diameter and particle diameter, respectively in cm. ρ_b is the density of the *flowing material* in g/cc. C_{FB} and k are constants. Within the range of granular material covered by Baverloo et al. (1961) it was found that the value of C_{FB} and k

are 35 and 1.4 respectively. In this model, the term ρ_b is difficult to measure. Baverloo suggested using the value of bulk density. It is often observed (Verghese and Nedderman, 1995) that fine particles undergo significant dilation due to interstitial pressure gradient and cannot be approximated by bulk density. As a result, the authors observed significant drop in flow rate. In other words, if bulk density is used in the equation 1, then constant of proportionality has to be different and it is function of particle diameter. The issue of arching is also not addressed in Baverloo's Equation (Nedderman et. al., 1982).

Recently, a numerical technique named discrete element method (DEM) is being widely used to simulate systems comprising of entities defined by a rigid boundary. The technique evolved from molecular dynamics simulation and Cundall and Strack (1979) first time applied it to granular system. DEM is also being employed by several research groups for material flow analysis in hopper (Cleary and Sawley, 2002, Langston et. al., 1996 and 2004; Li et al., 2004). Since all the calculations are done in an explicit manner the only limitation of the technique is computation time. Therefore, 2-dimensional calculations are preferable. However, it is possible to extend the technique in 3-dimension also. The numerical technique is described in detail in a later section.

The objective of the current research is to apply DEM for – 1) visualization of flow patterns of coarse material (10 mm size) for different hopper designs, 2) investigate the applicability of Baverloo's Model (Equation 1) for mass flow rate in conical and flat-bottom hoppers exclusively for very coarse material. At this point, the research was focused on numerical exercise only and experimental validation will be addressed in future.

DISCRETE ELEMENT METHOD (DEM)

The DEM refers to a numerical scheme that allows finite rotations and displacements of rigid bodies, where complete loss of contacts and formation of new contacts between bodies can occur as the calculation cycle progresses. Here, a brief description of the 2D DEM is given that is particularly useful to model interaction among spheres approximated as discs in 2-D. In the DEM given disc moves according to the forces acting on it. When a contact between two discs is detected, the collision is modeled by a pair of spring and dashpot, one in the normal direction and one in the tangential direction (Fure 1). In other words, the discs are allowed to overlap at the boundaries according to a contact model. The acceleration of the body is computed from the net force, which is then integrated for velocity and displacement. Referring to figure 1, every disc is identified separately, virtual overlap is allowed at each contact point, and the calculation is done for every disc in turn.

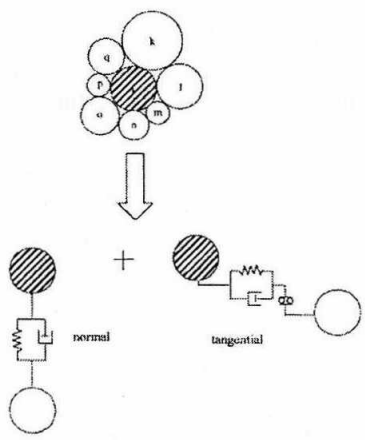

Fig. 1: Schematic Representation of an Assembly of Discs and the Spring-Dashpot Model in the Normal and Tangential Directions

The relative velocity of the disc i with respect to the discs in contact discs k, l, m, n, o, p, and q is first determined. These relative velocities for every contact of disc i are resolved in the normal direction along the line drawn through the centers of a pair of discs in contact and tangential direction and the force calculation is then done for each contact as follows:

$$\begin{aligned} \Delta F_n &= k_n v_n \Delta t \\ \Delta F_s &= k_s v_s \Delta t \\ \Delta d_n &= c_n v_n \\ \Delta d_s &= c_s v_s \end{aligned} \tag{2}$$

where, in an incremental time Δt, ΔF_n and ΔF_s are the incremental forces due to the springs, Δd_n and Δd_s are the incremental forces due to the dashpots, v_n and v_s are the relative velocities, and k and c are the spring stiffness and dashpot constant, respectively. Then, the contact forces and other body forces acting on the disc are vectorially summed to determine the net out-of-balance force acting on it. Other body forces such as drag, cohesive force, pressure may also be included in equation 2. However, this work is limited to interaction force among non-cohesive particle moving under gravity. The acceleration of disc i having mass m is given by:

$$\begin{aligned} \ddot{x}_i &= \frac{1}{m_i}\sum F_x \\ \ddot{y}_i &= \frac{1}{m_i}\sum F_y \\ \ddot{\theta}_i &= \frac{1}{I_{oi}}\sum M_o \end{aligned} \tag{3}$$

Where $\ddot{x}$ and $\ddot{y}$ are the acceleration in the x and y directions respectively, $\ddot{\theta}$ is the angular acceleration, I_{oi} the moment of inertia of the disc i, and M is the total moment acting on the disc. In light of the spring-and-dashpot model of collision, the tangential force due to the dashpot is limited by the maximum that can exist at the contact, which is given by:

$$F_{s,\max} = \mu . F_n \tag{4}$$

where m is the coefficient of friction and F_n is the normal force at the contact. If the absolute value of the tangential force in the spring-and-dashpot exceeds $F_{s,max}$, then slip is presumed to occur. In this situation, during the computation, the dashpot in the tangential direction is omitted and the F value is used instead

Equation 3 is numerically integrated to determine the velocity and then the displacement. Details of the numerical scheme are given in literature (Rajamani et al. 2000; Mishra and Rajamani, 1992; Cleary, 1998; Kawaguchi et al., 1998; Zhou et al. 2004). The stability of the calculation is dependent on the time step chosen. A stability analysis leads to –

$$\Delta t < 2\sqrt{m/k_n}$$

Since the model deals with individual contacts, it is necessary to get realistic values of the disc-to-disc and disc-to-wall contact properties. These parameters are material stiffness, coefficient of restitution, and coefficient of friction. Material stiffness property correctly establishes the forces generated in the spring. The coefficient of restitution is a measure of the damping property of the material, and hence it

figures in the dashpot constant of the material, which in turn establishes the forces developed in the dashpot. Rajamani et. al (2000) describes method to determine these material properties. For this investigation, model parameters published in literature (Djordjevic, 2005) for particles of similar size and density range were used. Typically, these parameters are also adjusted using experimental data.

In the current work, a 0.5 m x 1.0 m hopper was simulated with bottom part of various hopper-angles and orifice opening (Figure 2). The details of the simulation are given in the table 1.

Table 1: Material Properties and Simulation Details

Normal Stiffness	400,000 (N/m)
Shear Stiffness	300,000 (N/m)
Coefficient of restitution	0.45
Coefficient of friction	0.5
Particle Diameter	10 mm
Particle density	3000 kg/m^3
Particle number	3100
Hopper height	1.0 m
Hopper diameter	0.5 m
Hopper angles	44°, 60°, 90°, 120° and 180°
Orifice openings	20, 15, 10, 7.5, 6, 5, 4, 3 (cm)

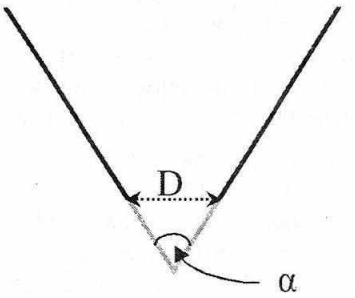

Fig. 2: Hopper Design. D = Orifice Opening and A = Hopper Angle

RESULTS AND DISCUSSIONS

In this investigation, only two design variables were considered. They are hopper angle (α) and orifice opening (D) as shown in figure 2.

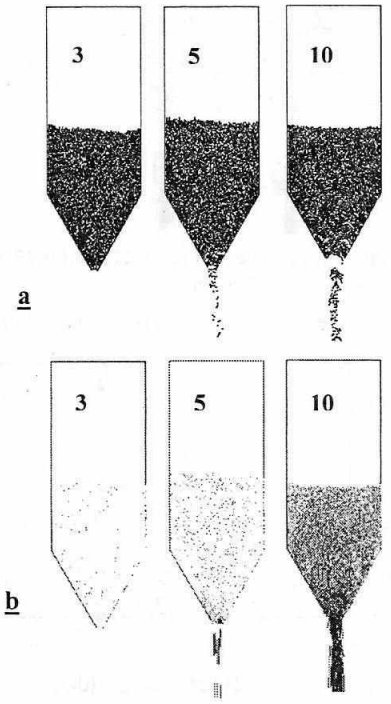

Fig. 3: Effect of Orifice Opening on - A) Particle Flow, B) Particle Velocity Profile. A = 60°

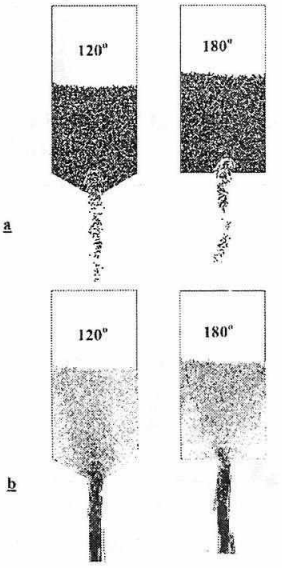

Fig. 4: Effect of Hopper Angle on - A) Particle Flow, B) Particle Velocity Profile. D = 10 cm

As expected, the flow gets constrained as the orifice opening reduces (Figure 3-a). For 3 cm opening the arching occurs after initial period of restricted flow. It was observed that irrespective of the hopper angle arching occurred at 3 cm orifice opening. Corresponding velocity profiles are shown in figure 3-b. The longer line denotes higher velocity. It is evident that when arching occurs the velocity of particles in the bulk nearly becomes zero. Minor velocity is observed in the image because particles are yet to reach rest position. For other two orifice opening, the velocity profiles correspond well with particle flow snapshots.

The effect of hopper angle on particle flow is shown in figure 3 and 4. Here hopper opening was kept at 10 cm and hopper angles were 60°, 120° and 180°. Relevant simulation for 60° hopper is already shown in figure 3. From the particle flow images the difference in flow pattern is not very significant. However, from the velocity profile images the presence of stagnant zone, as indicated by the white spots near the wall is very clear. The area of stagnant zone increases as the hopper angle increases.

The fluctuation of velocity profile is shown in figure 5. These simulation images were captured at a gap of 0.25 second between 1 and 2 seconds from the start of simulation. Darker spots in the bulk basically indicate the presence of higher velocity lines. These results verify non-fluid like behavior of granular mass. Particle mass accumulates at the orifice and then gets discharged and this phenomenon repeats in cycle. To smoothen out this fluctuation often secondary equipment such as vibratory feeders, screw feeders are used below a hopper. This fluctuation is minimized by proper design and usage of external vibrator strategically located on the hopper wall.

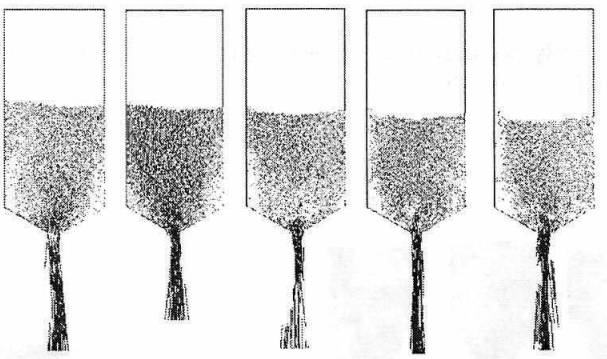

Fig. 5: Fluctuation of Velocity Profile Over Time. The Snapshots were Taken in Gap of 0.25 Second between 1 Sec and 2 Sec. A = 120° and D = 7.5 cm

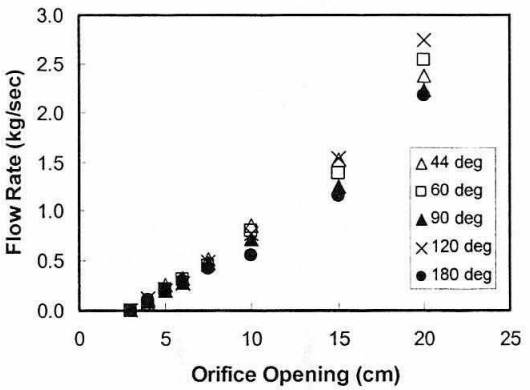

Fig. 6: Effect of Orifice Opening on Mass Flow Rate for Various Hopper Angles

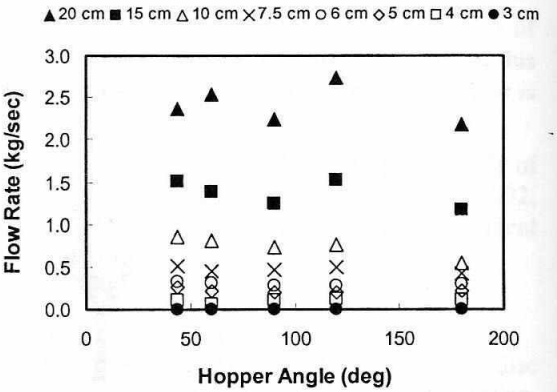

Fig. 7: Effect of Hopper Angle on Mass Flow Rate for Various Orifice Openings

Figure 6 and 7 presents variation of flow rates as function of orifice opening and hopper angle. As seen in DEM snap-shots, flow rate decreases with orifice opening. Orifice opening influences the flow rate to a greater extent than hopper angle. The effect of hopper angle for $D \geq 10$ cm. is not very distinct. The review article by Neddermann et al. (1982) states that for $\alpha > 90^{\circ}$ there is no effect of hopper angle on flow rate. This to a certain extent is evident in figure 6. A close observation reveals that for $\alpha < 90^{\circ}$ and $D \leq 10$ cm. a slight increase of flow rate is observed for steeper hoppers. For larger value of α, a stagnant boundary forms and only the core gets discharged (Figure 4-b). Therefore, the hopper angle does not influence the flow rate. The angle of this stagnant boundary is determined by the coefficient of internal friction between particles (Neddermann et al., 1982). The effect of hopper angle is a complex issue and requires further investigation.

The Baverloo model was revisited in the context of this numerical exercise and the results are shown in figure 8. Equation 1 suggests that a linear plot between $W^{2/5}$ and D will results in a straight line. The results of this work are plotted in figure 8 along with the calculated values using parameters suggested by Baverloo et al. (1961). Also, it is to be noted that the density of the flowing material was taken as the bulk density, which was calculated assuming 40% voidage (1.8 g/cc). There is significant disagreement between Baverloo Model results and DEM simulation predictions. Baverloo Model predictions are higher than that of DEM results and this mismatch increases with orifice opening. One of the critical parameters of Baverloo model is the density of flowing material, which is difficult to estimate. The value of the model parameter C_{FB} depends on this density value (Neddermann et al, 1982).

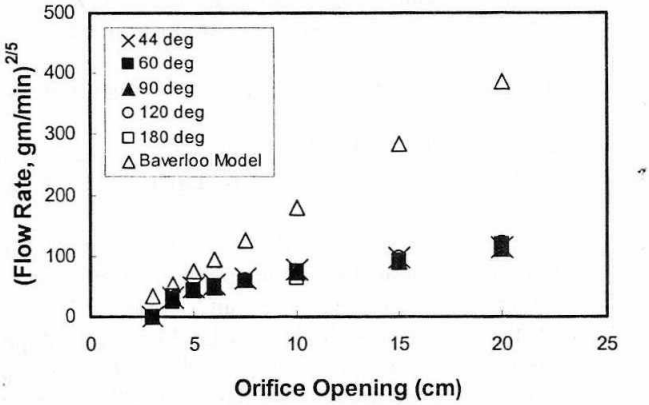

Fig. 8: Baverloo Plot for Coarse Particle Flow in Hopper Calculated From DEM Simulations

Figure 8 also shows that the DEM results do not lie on a single straight line. On the contrary the curve can be divided on two segments of straight line with different slopes. According Baverloo model the limiting orifice size should be equal to $k.d$, i.e. 1.4 cm. But the arching and flow blockage was observed at 3.0 cm. Verghese and Neddermann (1995) published further evidence that the value C_{FB} of Bavreloo Equation needed to be modified for fine sands. So in other words it appears that although flow rate is proportional to $D^{5/2}$, but model parameters may be different as the particles undergo a flow regime shift when the orifice size is decreased. Neddermann et al. (1982) has pointed out that flow behavior significantly alters when $D < 6.d$ and at that range validity of original Baverloo Model is questioned. It is reminded that in this exercise the particle size (10 mm) is quite large.

In any case, Baverloo's Model provides a good foundation based on which similar relationship for particles of varying properties can be developed. Further work will be carried out in this area which includes experimental validation of DEM simulation and effect of particle size distribution on the flow rate. Also, it is intended to investigate the relationship between flow rate and orifice-to-particle diameter in detail.

CONCLUSIONS

Flow of particulate material in a hopper is investigated using discrete element method (DEM). The study was focused on understanding flow of coarse material of 10 mm size. DEM simulation could pick up anomalous phenomena such as arching. The presence of stagnant boundary was also indicated for shallow hoppers. Also, the fluctuation of material flow, which is an undesirable occurrence, could be visualized.

Baverloo Model correlating particle flow rate and orifice size was re-examined. The proportionality relation between Flow rate, W and (orifice size, $D)^{5/2}$ is still valid for coarse particle range. However, it is possible that the constant of proportionality are different for this size of particle. Furthermore, perhaps a point of inflexion exists at $D = 6.d$, where this proportionality constant changes.

In future, experimental validation will be conducted to substantiate these results. Besides, the effect of particle size distribution, particle density and orifice-to-particle size ration on flow rate will be investigated in detail.

REFERENCES

[1] Baverloo, W. A., Leninger, H. A., and van de Vande, J., 1961, "The flow of granular solids through orifice", Che. Eng. Sci., 15, pp. 260-269

[2] Cleary, P.W., 1998. "Predicting charge motion, power draw, segregation and wear in ball mills using discrete element methods", Miner. Eng. 11 (11), pp.1061– 1080.

[3] Cundall, P.A., Strack, O.D.L., 1979. "A discrete numerical model for granular assembly", Geotechnique 29, pp. 47– 65.

[4] Djordjevic, N., 2005, "Influence of charge size distribution on net-power draw of tumbling mill based in DEM modeling", 18 (3), pp. 375-378.

[5] Kawaguchi, T., Tanaka, T., and Tsuji, Y., 1998, "Numerical simulation of two-dimensional fluidized beds using the discrete element method (comparison between the two- and three-dimensional models)", 96, pp. 129-138.

[6] Langston, P. A., Tüzün, U., and Heyes, D. M., 1996, "Distinct element simulation of interstitial air effects in Axially symmetric granular flows in hoppers", Che. Eng. Sci., 51 (6), pp. 873-891

[7] Langston, P. A., Al-Awamleh, M. A., Fraige, F. Y., and Asmar, B. N., 2004, "Distinct element modeling of non-spherical frictionless particle flow", Che. Eng. Sci., 59, pp. 425-435.

[8] Li, J., Langston, P. A., Webb, C., and Dyakowski, T., 2004, "Flow of sphero-disc particles in rectangular hoppers – a DEM and experimental comparison in 3D", Che. Eng. Sci., 59, pp. 5917-5929.

[9] Jenike, A. W., 1964, "Storage and flow of solids", Bulletin No. 123, Utah Engineering Experiment Station, University of Utah.

[10] Mishra, B.K., Rajamani, R.K., 1992. "The discrete element method for the simulation of ball mill" Appl. Math.Model. 16, pp.598– 604.

[11] Nedderman, R. M., Tüzün, U., Savange, S. B., and Houlsby, G. T., 1982, "The flow of granular material-1", Che. Eng. Sci., 37 (11), pp. 1597-1609.

[12] Rajamani, R.K., Mishra, B.K., Venugopal, R., Datta, A., 2000. "Discrete element analysis of tumbling mills", Powder Tech., 109 (1– 3), pp. 105– 112.

[13] Verghese, T. M. and Nedderman, R. M., 1995, "The discharge of fine sands from conical hoppers", Che. Eng. Sci., 50 (19) pp. 3142-3153.

[14] Zhou, Y.C.; Yu, A.B.; Stewart, R. L.; Bridgwater, J.; "Microdynamic analysis of the particle flow in a cylindrical bladed mixer", Che. Eng. Sci., 59, pp. 1343-1364.

NOMENCLATURES

c_n	Normal dashpot constant	y	Displacement in y-direction
c_s	Shear dashpot constant	C_{FB}	Constant
d	Particle diameter	D	Orifice diameter
d_n	Normal force due to dashpot component	F_n	Normal force due to spring component
d_s	Shear or tangential force due to dashpot component	F_s	Shear or tangential force due to spring component
g	Acceleration due to gravity	I	Moment of inertia
k	Constant	M	Moment
k_n	Normal stiffness (N/m)	W	Mass flow rate, g/min
k_s	Shear stiffness (N/m)	θ	Angular displacement
v_n	Normal relative velocity	ρ_b	Bulk density, g/cc
v_n	Shear relative velocity	μ	Coefficient of friction
x	Displacement in x-direction		